Biosensors and Bioelectronics 31 (2012) 316–322

Contents lists available at SciVerse ScienceDirect

Biosensors and Bioelectronics

journal homepage: www.elsevier.com/locate/bios

Contribution of potassium ion and split modes of G-quadruplex to the sensitivity and selectivity of label-free sensor toward DNA detection using fluorescence

Jiangtao Ren[a,b], Jiahai Wang[a,*], Jin Wang[a,c,*], Nathan W. Luedtke[d], Erkang Wang[a,*]

[a] State Key Laboratory of Electroanalytical Chemistry, Changchun Institute of Applied Chemistry, Chinese Academy of Sciences, Changchun, Jilin 130022, China
[b] Graduate School of the Chinese Academy of Sciences, Beijing 100039, China
[c] Department of Chemistry and Department of Physics, State University of New York at Stony Brook, New York 11794, USA
[d] Institute of Organic Chemistry, University of Zürich, Winterthurerstrasse 190, Zürich CH-8057, Switzerland

ARTICLE INFO

Article history:
Received 8 September 2011
Received in revised form 16 October 2011
Accepted 19 October 2011
Available online 25 October 2011

Keywords:
Split G-quadruplex
DNA sensor
Label-free
Single mismatch
Fluorescent probe

ABSTRACT

In recent years, bioanalytical technology based on G-quadruplex has been paid significant attention due to its versatility and stimulus-responsive reconfiguration. Notwithstanding, several key issues for template-directed reassembly of G-quadruplex have not been resolved: what is the key factor for determining the sensitivity and selectivity of split G-quadruplex probes toward target DNA. Therefore, in this study, we designed three pairs of split G-quadruplex probes and investigated the sensitivity and selectivity of these systems in terms of potassium ion concentration and split modes of G-quadruplex. Due to its simplicity and sensitivity, N-methyl-mesoporphyrin (NMM) as fluorescence probes was used to monitor the target-directed reassembling process of G-quadruplex. A G-quadruplex sequence derived from the c-Myc promoter was split into "symmetric" probes, where each fragment contained two runs of guanine residues (2 + 2), or into "asymmetric" fragments each containing (3 + 1 or 1 + 3) runs of guanine residues. In all three cases, the sensitivity of target detection was highly dependent on the thermodynamic stability of the hybrid structure, which can be modulated by potassium ion concentrations. Using a combination of CD, fluorescence, and UV spectroscopy, we found that increasing potassium concentrations can increase the sensitivity of target detection, but can decrease the selectivity of discriminating cognate versus mismatched "target" DNA. The previous argument that asymmetrically split probes were always better than symmetrically split probes in terms of selectivity was not plausible anymore. These results demonstrate how the sensitivities and selectivity of split probes to mutations can be optimized by tuning the thermodynamic stability of the three-way junction complex.

1. Introduction

Nowadays, the specific detection of nucleic acid sequences has attracted widespread efforts in modern life science (Wang et al., 2009). Most methods such as, electrochemistry (Bonanni et al., 2010; Ferapontova et al., 2010; Hejazi et al., 2010; Li et al., 2010a), colorimetry (Bai et al., 2010; Kim et al., 2010; Qin et al., 2010b; Song et al., 2010), SPR (D'Agata et al., 2010) or fluorescence (Guo et al., 2009; Häner et al., 2010; Tyagi and Kramer, 1996), have been constructed based on hybridization between a probe DNA and complementary "target" sequence followed by signal amplification and detection. These methods typically require covalent modification(s) of the DNA to carry different tags, such as gold or silver nanoparticles (Li and Rothberg, 2004), quantum dots (Russ Algar et al., 2009; Wang et al., 2010; Zhang and Hu, 2010), redox–active metal complexes, biotin, or fluorescent dyes (Häner et al., 2010; Yang et al., 2005). The requisite covalent conjugation step results in extra cost and time needed for the analysis. To surmount this limitation, non-covalent labelling and detection strategies are being developed (Elbaz et al., 2009; Pavlov et al., 2004; Xiao et al., 2004). Several groups have demonstrated that the re-folding of split G-quadruplex sequences can be promoted by their hybridization to a DNA target sequence that is complementary to the regions surrounding the G-quadruplex motif (Deng et al., 2008; Kolpashchikov, 2008, 2010; Nakayama and Sintim, 2009; Qiu et al., 2011). For example, Kolpashchikov used a symmetrically split peroxidase DNAzyme to visualize single nucleotide polymorphisms using a colorimetric assay (Kolpashchikov, 2008). Later, Zhou developed an asymmetrically split G-quadruplex with 3:1 mode to detect target DNA with a detection limit in the nanomolar range (Deng et al., 2008). To optimize the parameters of such G-quadruplex-based sensors, Sintim and co-workers evaluated various probe architectures and

* Corresponding authors at: State Key Laboratory of Electroanalytical Chemistry, Changchun Institute of Applied Chemistry, Chinese Academy of Sciences, Changchun, Jilin 130022, China. Tel.: +86 431 85262003; fax: +86 431 85689711.
E-mail addresses: jhwang@ciac.jl.cn (J. Wang), jin.wang.1@stonybrook.edu (J. Wang), ekwang@ciac.jl.cn (E. Wang).

0956-5663/$ – see front matter © 2011 Elsevier B.V. All rights reserved.
doi:10.1016/j.bios.2011.10.038

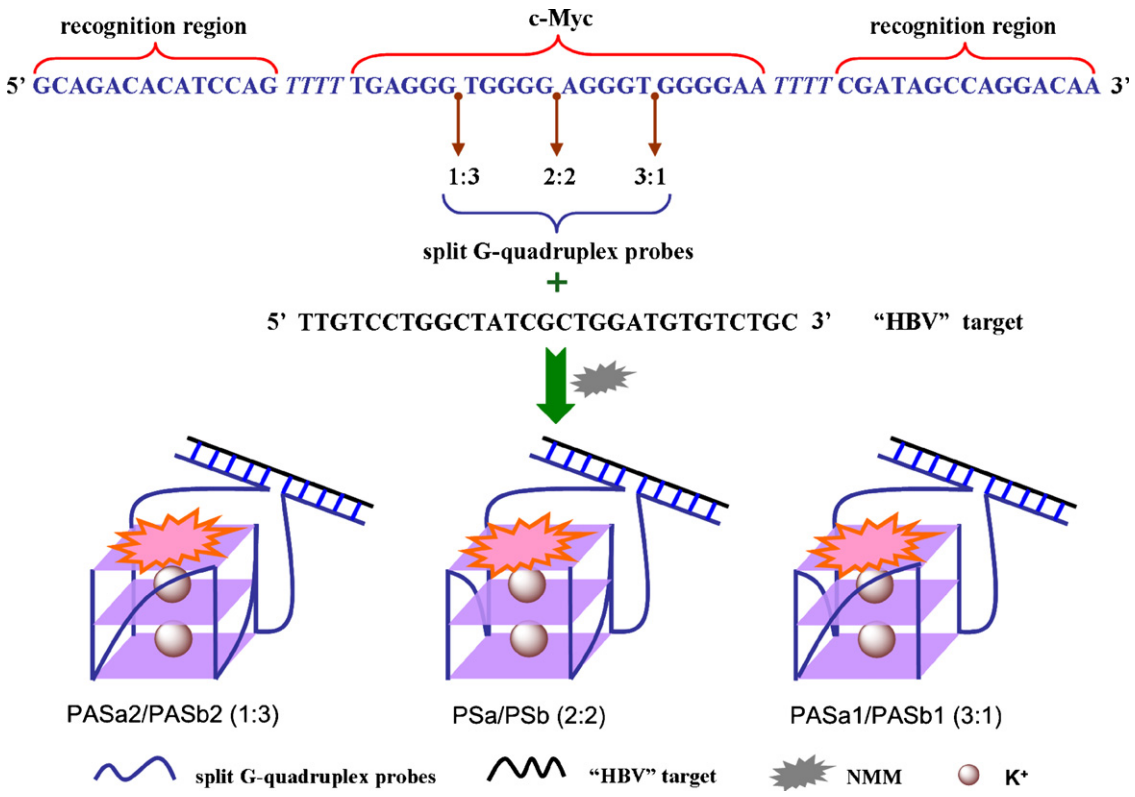

Scheme 1. Designed scheme of split G-quadruplex probes in different split modes and hybridization between the probes and target DNA promoting formation of G-quadruplex, which binds NMM, and intensifies its fluorescence, in the presence of potassium ion.

reaction conditions (Deng et al., 2008; Kolpashchikov, 2008, 2010; Nakayama and Sintim, 2009; Qiu et al., 2011), and the nature of monovalent ion was found to be a key determinant of the proficiency of peroxidase-mimicking G-quadruplex. However, the use of H_2O_2 and other reactive oxygen species by peroxidase-mimicking G-quadruplexes might introduce oxidative damage into these systems that negatively impact reproducibility (Vialas et al., 2000). In terms of stability and reproducibility, small molecules with enhanced fluorescence upon G-quadruplex binding can provide new opportunities for improved label-free detection of nucleic acids. Examples of fluorescent G-quadruplex ligands include derivatives of ethidium (Koeppel et al., 2001), carbazoles (Chang et al., 2004), platinum–dipyridophenazine complexes (Ma et al., 2009), bisquinolinium/thiazole orange conjugates (Yang et al., 2009), phthalocyanines (Alzeer et al., 2009), and porphyrins (Hu et al., 2010; White et al., 2007). More recently, in one of our previous studies (Ren et al., 2011), two kind of biosensors based on a symmetrically split G-quadruplex and G-quadruplex-specific dyes were designed and capable of detection of perfectly matched DNA with a detection limit in the nM range.

However, information gleaned from these colorimetric and fluorometric experiments did not allow us to understand the key determinants of split probe design in terms of optimized selectivity for cognate over mismatched DNA. A systematic study of relevant parameters was therefore required. Here we report three basic design strategies for splitting a stable G-quadruplex sequence derived from the c-Myc promoter (Phan et al., 2004; Qin and Hurley, 2008). As this sequence contains four runs of guanine residues, probes were generated by dissections at positions that resulted in one, two, or three tracts of guanine residues in each strand (Scheme 1 and Table S1). As a test "target", the regions flanking the split quadruplex were made complementary to a biologically important target DNA sequence ("HBV" target) derived from the hepatitis B virus (Weizmann et al., 2008). One porphyrin derivative, N-methyl mesoporphyrin IX (NMM) (Fig. S1), which can selectively bind to G-quadruplex instead of double-stranded and single-stranded DNA with the result of its fluorescence enhancement (Arthanari et al., 1998), was utilized as fluorescent probe to indicate the formation of G-quadruplex. According to circular dichroism (CD), UV–vis spectroscopy and fluorescence spectroscopy, all three pairs of split probes exhibited DNA target-dependent and potassium-dependent re-folding into G-quadruplex structures that were capable of binding NMM to generate fluorescent complexes. Interestingly, symmetrically split probes containing 2 + 2 G-tracts were better suited for detecting single-point mutations in target sequences as compared to both of the asymmetrically split G-quadruplex probes (3 + 1 and 1 + 3 G-tracts). These results are in sharp contrast to previous results obtained using peroxidase-based assays that suggested asymmetrically split probes are superior (Deng et al., 2008). To investigate the origin of this effect, we used thermal denaturation to determine the relative stabilities of each pair of split probes and target DNA as a function of potassium chloride concentration. Increasing potassium concentrations increased the thermodynamic stabilities of the hybrids and improved the sensitivity of the split probes for target DNA, but at high salt concentrations a loss of selectivity for cognate versus mismatched DNA was observed. At the same concentration of salt, the stability of hybrids of probes and target DNA was found to be in the order: symmetrically split probes (2 + 2) > asymmetrically split probes (1 + 3) > asymmetrically split probes (3 + 1). Each pair of probes has its own best working condition in terms of selectivity. Under optimized potassium concentrations of 1 mM, the symmetrically split (2 + 2) probes can selectively discriminate single-base mismatch DNA from the perfectly matched target DNA even in diluted biological fluids such as urine. Due to their lower thermodynamic stabilities, asymmetrically split probes (1 + 3) and (3 + 1) exhibited higher optimal potassium concentrations of 10 mM and 50 mM, respectively. These results demonstrate how co-variation of probe

design and potassium concentration is intimately linked parameters in G-quadruplex-mediated fluorescent readouts of duplex hybridization.

2. Materials and methods

2.1. Materials

HPLC-purified oligonucleotides (Table S1) and tris(hydroxymethyl)aminomethane (Tris) were obtained from Sangon Biotechnology Co., Ltd (Shanghai, China). N-methyl mesoporphyrin IX (NMM) was purchased from Frontier Scientific, Inc. (Logan, UT, USA). Potassium chloride was purchased from Sinopharm Group Chemical Reagent Co., Ltd. (Shanghai, China). The oligonucleotides were dissolved in Tris buffer (Tris–OAc 25 mmol/L, pH 7.4) and quantified using UV–Vis absorption spectroscopy with a Cary 500 UV–vis–NIR spectrometer (Varian). All oligonucleotides were stored at −20 °C and were heated to 95 °C for 5 min and gradually cooled to room temperature immediately before use. Stock solutions of NMM (5 mmol/L) were prepared in DMSO, stored in the dark at −20 °C, and diluted to the required concentration with Tris buffer. All reagents were used as received without further purification. Double distilled water was used throughout.

2.2. Apparatus and parameters

Absorption measurements were performed with a Cary 500 UV–vis–NIR spectrometer (Varian). Fluorescence spectra were recorded on a Perkin-Elmer LS 55 luminescence spectrometer at 20 °C, utilizing slits of 5/15 nm, a scan rate of 500 nm/min, excitation at 399 nm, and emission at 611 nm. Circular dichroism (CD) spectra were collected using a JASCO J-820 spectropolarimeter (Tokyo, Japan).

2.3. Circular dichroism measurements

Each background corrected CD spectrum was collected using 1 μmol/L of each split probe, 1 μmol/L HBV targets and variable concentrations of K^+. Samples were prepared as follows: 80 μl HBV target (10 μmol/L), 80 μL of each split probe (10 μmol/L) and K^+ were mixed successively; the mixture was adjusted to 800 μL and incubated for 1 h at 20 °C. CD measurements from 210 to 350 nm were taken, the data pitch was 0.1 nm, scan speed was 200 nm/min, response time was 0.5 s, and bandwidth was 1 nm.

2.4. Thermal melting experiments

Aforementioned samples were covered with mineral oil. The absorbance of each sample was monitored at 260 nm as a function of temperature while ramping at a rate of 1 °C/min. The T_m of each DNA sample was determined using first derivative analysis by the data-processing software of Origin 7.5.

2.5. DNA–NMM complex preparation and analysis

Solutions containing 1 μmol/L NMM, 1 μmol/L of each split probe, and the indicated K^+ concentration were prepared with or without 1 μmol/L HBV target, and incubated for 1 h at 20 °C. The Soret band of NMM was recorded using UV–vis spectrophotometer. The binding of split probes to NMM was demonstrated according to the hyperchromicity of the NMM Soret band.

2.6. Fluorometric assays of perfectly matched versus mismatched "HBV" targets

Three single-base mismatched targets (SM-15, SM-9 and SM-22) and a three-base mismatched target (TM) were evaluated (sequences shown in Table S1). Generally, 50 μL of mismatched targets or perfectly matched target (1 μmol/L), 50 μL of each split probe (2 μmol/L), and 50 μL of NMM (10 μmol/L) were mixed with indicated concentrations of K^+ and adjusted up to 500 μL with 25 mmol/L Tris buffer solution (pH 7.4). The mixtures were incubated for 1 h at 20 °C prior to the quantification of NMM fluorescence using excitation at 399 nm and emission at 611 nm.

2.7. "HBV" target titration and applicability in the 1% urine

500 μL Solutions containing 1 μmol/L NMM, 200 nmol/L of each symmetrically split probe, and various concentrations of "HBV" target were incubated in the presence of 1 mmol/L K^+ for 1 h at 20 °C and fluorescent spectra were collected. To test the applicability of our system, human urine was used. The urine was centrifuged at 8000 rpm for 5 min, and the supernatant was diluted with Tris buffer. 500 μL Tris buffer containing 1 μmol/L NMM, 200 nmol/L of each symmetrically split probe, 100 nmol/L of "HBV" target and 1% urine were prepared with 1 mmol/L K^+.

3. Results and discussion

3.1. Potassium ion dependent fluorescence readout of three split modes

Scheme 1 depicts our general design of DNA-templated reconstitution of an intermolecular G-quadruplex that binds to NMM to provide fluorescence readout of hybridization. In this example, each pair of split G-quadruplex probes is derived from the c-Myc promoter (Scheme 1 and Table S1) (Qin and Hurley, 2008). The split probes fragments are reconstituted into G-quadruplexes upon addition of an arbitrary "HBV" target DNA, resulting in a G-quadruplex-specific enhancement in NMM fluorescence. Monovalent cations, especially potassium, stabilize the G-tetrads of G-quadruplex structures (Hud et al., 1996; Sen and Gilbert, 1990; Xu et al., 1993). It was therefore important to characterize the effect of potassium on the duplex-mediated reassembly of split G-quadruplex probes. For convenience, we define a fluorescent enhancement factor (EF) of NMM as $EF = S_x/S_0$, where S_x and S_0 are the background-corrected fluorescence intensity of NMM in the presence and absence of target, respectively. To evaluate the potassium-dependence and specificity of NMM fluorescence enhancements, we conducted potassium titrations in the absence and presence of "HBV" target DNA. As shown in Fig. 1, the fluorescence intensity of NMM in the presence of the symmetrically split probes (PSa/PSb, 2:2) lacking target DNA did not increase with K^+ concentration (curve 1). In the presence of target DNA, however, the fluorescence of NMM dramatically increased and reached a plateau at potassium concentrations of 10 mM and above (curve 6). Similar results were obtained using the asymmetrically split probe (PASa2/PASb2, 1:3; and PASa1/PASb1, 3:1) except that 50 mM and 150 mM KCl were needed to saturate their fluorescence changes (Fig. S2), respectively. These data suggested that reconstituted G-quadruplex based on symmetrically split probes had a higher stability and NMM binding affinity as compared to the asymmetric ones. For the three split probe designs (PSa/PSb, PASa2/PASb2 and PASa1/PASb1), the EF values reached the approximate maximum values of 3, 3.5 and 3 at KCl concentrations of 10, 50 and 150 mM, respectively.

3.2. Characterization of hybrids by UV and CD

Previous studies have demonstrated that variable potassium concentrations can influence the conformation and stability of G-quadruplexes and impact their affinities for fluorescent dyes

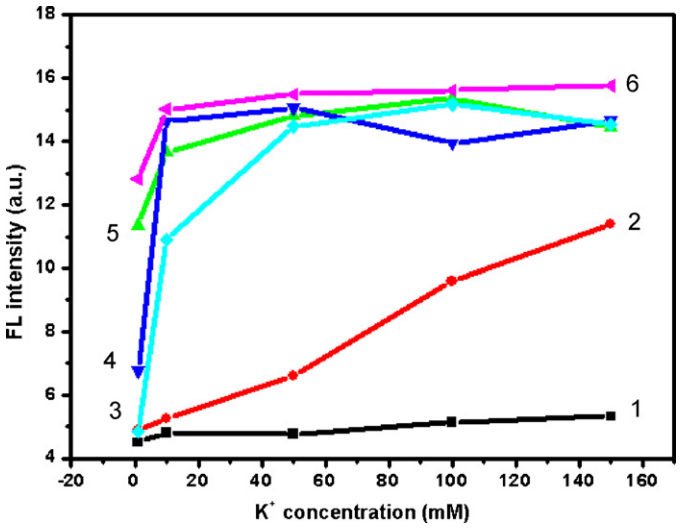

Fig. 1. Fluorescent detection of mismatches using symmetrically split G-quadruplex probes. The graph represents the fluorescence intensity of each sample at emission wavelength of 611 nm as function of K^+ concentration. Curve 1 is NMM + split probes only; curve 6 is NMM + split probes plus + perfectly matched target; curve 2 is NMM + split probes + TM; curve 3 is NMM + split probes + SM-22; curve 4 is NMM + split probes + SM-9; and curve 5 is NMM + split probes + SM-15. Experimental conditions: 1 μM NMM, 200 nM of each split probe, 100 nM "HBV" targets if any, and K^+ of different concentration in 25 mM Tris buffer solution (pH 7.4).

(Li et al., 2010b; Qin et al., 2010a). To investigate how variable potassium concentrations can affect the conformations of G-quadruplex-duplex hybrid (three-way junction) structures, CD spectra were collected as a function of KCl concentration (Figs. 2A and S3). For all three groups of split probes in the presence of target DNA, an enhanced signal at 265 nm and 243 nm were observed upon addition of KCl, indicating formation of "parallel" G-quadruplex structures at the three-way junction of each hybrid. These CD features are consistent with those of the c-Myc promoter DNA sequence that is known to adopt a parallel conformation in solution (Fig. S4) (Phan et al., 2004; Qin and Hurley, 2008). Similar to the potassium-dependent trends in NMM fluorescence (Fig. 1) the changes in ellipticity of symmetrically split (2 + 2) probes and target DNA reached a plateau at 1 mM of KCl and above (Fig. 2B).

Table 1
(A) T_m values of melting the three-way junctions from hybridization between split probes and perfectly matched "HBV" target in the presence of variable potassium concentration. (B) T_m values of melting the three-way junctions from hybridization between split probes and targets (Note: C(K^+) means the concentration of potassium ion in each sample. The melting profiles were shown in the Figs. S6 and S11).

T_m(°C)	l mM K^+	l0 mM K^+	50 mM K^+	150 mMK^+
A				
PSa/PSb (2:2)	42.9	46.0	52.0	59.0
PASa2/PASb2 (1:3)	41.0	45.0	51.0	58.0
PASal/PASbl (3:1)	40.0	43.0	49.0	57.0

T_m(°C)	C(K^+)	"HBV"	SM-15	SM-9	SM-22
B					
PSa/PSb (2:2)	l mM	44.0	41.5	36.0	38.0
PASa2/PASb2 (1:3)	10 mM	45.0	44.0	39.0	39.0
PASal/PASbl (3:1)	50 mM	49.0	47.0	46.0	46.0

For asymmetrically split probes PASa2/PASb2 (Fig. S3A and B) and PASa1/PASb1 (Fig. S3C and D), higher KCl concentrations of 10 mM and 50 mM, respectively, were needed to saturate the ellipticity changes. In addition, similar CD titrations were carried out in the presence of NMM, and the analogous potassium-dependent trend of ellipticity changes was obtained (Fig. S5, for PASa2/PASb2), suggesting that the optimal KCl concentrations upon addition of NMM to saturate the ellipticity changes were similar. A correlation between potassium-dependent G-quadruplex stabilization and NMM fluorescence enhancement is therefore apparent.

To evaluate the impact of probe design and potassium concentration on the thermodynamic stabilities of these hybrids, UV melting experiments were conducted (Fig. S6). According to the melting profiles at 260 nm in Fig. S6A–D and corresponding differential curves in Fig. S7, the melting processes of the G-quadruplex and duplex are cooperative (Nakayama and Sintim, 2009), and melting temperatures (T_m) for hybrid of symmetrically spit probes and target DNA at 1 mM, 10 mM, 50 mM and 150 mM concentration of potassium were calculated and shown in Table 1A. The T_m values for symmetrically split probes were all slightly higher ($\Delta\Delta T_m$ = +1 to +3 °C) than those of asymmetrically split probes at the same potassium concentration, which indicted that hybrid of symmetrically split probes and target DNA was more stable than the hybrid of asymmetrically split probes and target DNA.

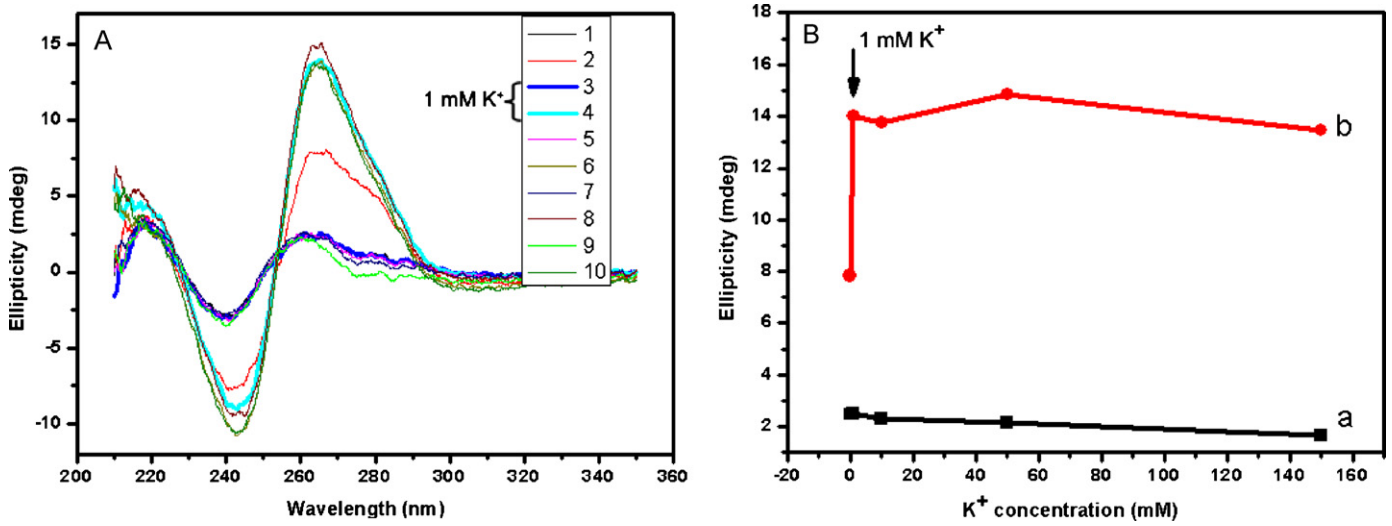

Fig. 2. (A) Potassium-dependent CD spectra of symmetrically split G-quadruplex probes without (odd number) or with (even number) "HBV" targets in the presence K^+ of different concentration; (B) The ellipticity of each sample at 265 nm as function of K^+ concentration without (a) or with (b) "HBV" targets. Experimental condition: 1 μM of each split probe, 1 μM HBV targets, 0 mM K^+ for curves 1 and 2, 1 mM K^+ for curves 3 and 4, 10 mM K^+ for curves 5 and 6, 50 mM K^+ for curves 7 and 8, and 150 mM K^+ for curves 9 and 10, in 25 mM Tris buffer solution (pH 7.4).

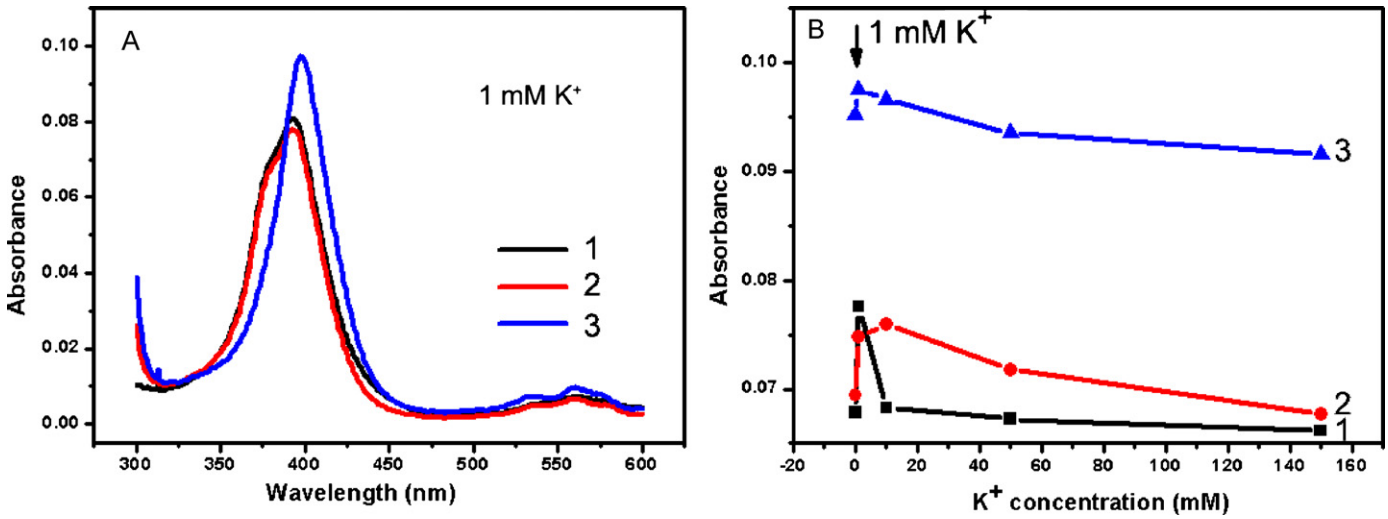

Fig. 3. (A) UV–vis spectra of NMM in the presence of symmetrically split G-quadruplex probes without (2) or with (3) "HBV" targets in the presence1 mM K^+; (B) absorbance of each sample at 397 nm as function of K^+ concentration without (2) or with (3) "HBV" targets. Curve 1 represents NMM only; curve 2 is NMM plus split probes, and curve 3 is a mixture of NMM, split probes and "HBV" target DNA. Experimental condition: 1 μM NMM, 1 μM of each split probe and 1 μM HBV targets in 25 mM Tris buffer solution (pH 7.4).

It has to be noted that the global stability of each hybrid was quite similar at any given potassium concentration (Table 1A), suggesting a dominating role of duplex formation as the main energetic driving force for hybridization at potassium concentrations. Only slightly higher T_m values were observed for the symmetric (2 + 2) split probe design as compared to the asymmetric designs (3 + 1 and 1 + 3), even in the presence of 1 mM K^+, where the asymmetrically split probes cannot assemble and fold into the G-quadruplex. This suggests a relatively small and similar contribution by each G-quadruplex to the overall thermodynamic stability of each hybrid. A dominant energetic role played by the hybridization of the duplex regions is likely to be an important pre-requisite for sensitive detection of single-base mismatches within these same duplex regions.

CD measurements directly provided information about the G-quadruplex while UV measurements can directly provide the clues about what happened to NMM. These two techniques offer us the complementary insights into this new label-free biosensor platform. To gain better insight into the potassium-dependent interactions between NMM and each split hybrid structure, absorbance spectra of NMM were collected as a function of potassium concentration. As indicated in Fig. 3A, the addition of symmetrically split probes into Tris buffer solution containing 1 mM potassium and NMM induced only slight changes in the absorption peak of NMM at 393 nm, whereas the absorption peak of NMM shifted to 397 nm upon addition of the probes and target DNA. For all three groups of split probes the minimal potassium concentration needed to induce maximum absorption of NMM (Figs. 3B and S8) coincided with the concentration needed for the maximal change in ellipticity (Figs. 2 and S3). These UV measurements therefore confirm that the NMM binding and fluorescence enhancements depend directly on the formation of G-quadruplex structures at the three-way junction of each hybrid construct. These results also suggest that the three pairs of split probes each have an optimal potassium concentration where they can exhibit maximal enhancement effectors (EF) and highest sensitivity to "HBV" target.

The conditions for highest sensitivity, however, do not necessarily correlate with optimal conditions for good selectivity in detecting proper versus improper base pairing within the duplex regions. Although split probes PSa/PSb (2 + 2) had highest stability as compared to other two pairs of asymmetrically split probes, asymmetrically split probes PASa2/PASb2 (1:3) under the condition of 50 mM potassium had the best sensitivity in terms of EF value (3.5). As shown in Fig. S9, Calibration curve based on asymmetrically split probes PASa2/PASb2 (1:3) showed detection limit of 0.1 nM (S/N = 5). Although the split probes (PASa2/PASb2) exhibited unobservable response toward TM, indicated by the indistinct change of fluorescence intensity upon addition of TM into the solution containing NMM + probes, single-point mutations could not be identified very well from perfectly matched target (Fig. S2A), in the presence of 50 mM K^+.

3.3. Potassium ion dependent selectivity of split probes for target DNA against point mutations

"HBV" replication results in random mutations that can convey resistance to antiviral medicines and may accelerate the carcinogenesis process (Kuang et al., 2004). To evaluate the selectivity of our split probe designs for mutations in the "HBV" target sequence, we selected three different single-base mismatches (SM-15, SM-9 and SM-22), located at positions 15, 9 and 22 from 5′-end of the "HBV" sequence (Table S1). To determine the best working conditions for each pair of split probes in terms of selectivity, potassium titrations into solutions containing split probes and mutated target DNAs were conducted (Figs. 1 and S2). The fluorescence intensities of each sample increased with increasing potassium concentrations, but the differences between cognate and mismatched DNA dramatically decreased at high concentrations of potassium. The best working conditions for each pair of split probes therefore required a balance between sensitivity and selectivity. The symmetrically split probes can discriminate single-base mismatch DNA in 1 mM KCl (Fig. 1), while the asymmetrically split probes (1 + 3) and (3 + 1) exhibited optimal potassium concentrations of 10 mM and 50 mM, respectively (Fig. S2), where stable G-quadruplexes can just form. CD and thermal stability data collected at these optimimal potassium concentrations reveal a correlation between the ellipticity values and fluorescence intensities. For example, for the symmetrically split probes, the single-point mutant "SM-22" was the most detrimental to NMM fluorescence intensity (Fig. 1, curve 3) and ellipticity (Fig. S10A), and SM-9 also had a large impact on each factors, while SM-15 had the little impact.

The melting temperature for each sample was derived from differentiating the melting profile (Fig. S11) and was listed in Table 1B. For the three split designs, the melting temperatures for hybrid containing SM-9 and SM-22 were lower than that corresponding to

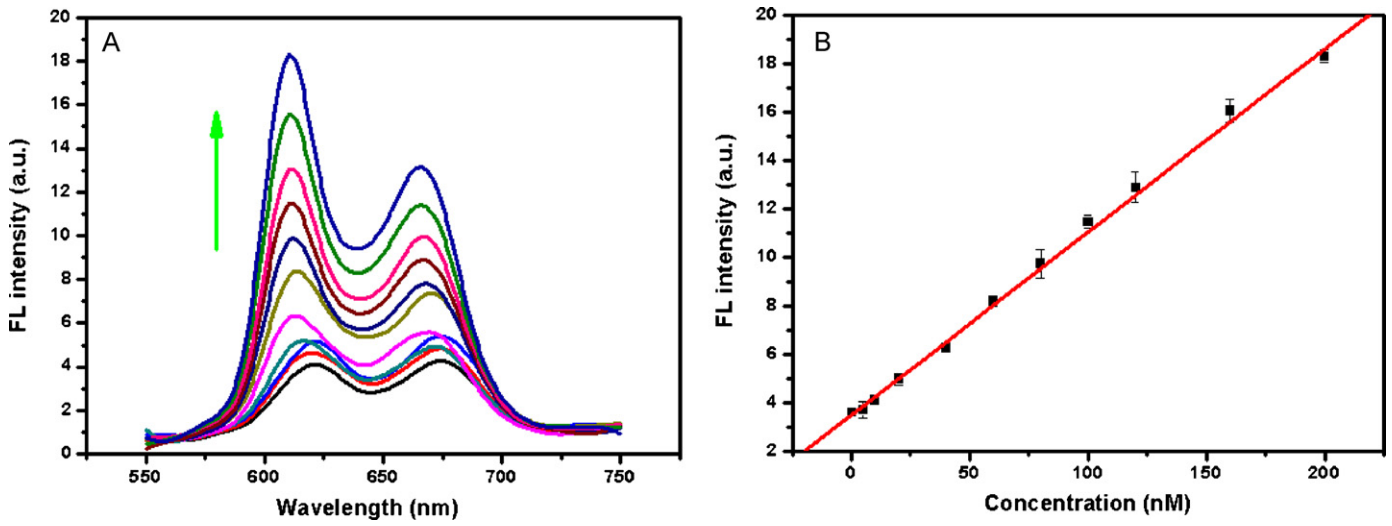

Fig. 4. Fluorescent response of NMM + symmetrically split G-quadruplex probes as function of concentration of "HBV" target concentration: 0, 5, 10, 20, 40, 60, 80, 100, 120, 160 and 200 nM. The error bars indicates the standard deviation of three repeated measurements for each concentration of target DNA. Experimental conditions: 1 μM NMM, 200 nM of each split probe (PSa/PSb), and 1 mM K^+, in Tris buffer solution (pH 7.4).

SM-15. These results indicate that mutants located near the center of each duplex region can be detected with much greater sensitivity than single-nucleotide polymorphisms located near the center of the target sequence. These results are consistent with the dominant energetic role of duplex hybridization.

Our comparison of split probe design has revealed that the symmetrically split probes (2:2) offer the best selectivity at 1 mM concentration of potassium. We therefore chose this pair of split probes to evaluate the potential of this approach as a practical analytical method (Fig. 4). A calibration curve evaluating the fluorescence enhancement of NMM upon titration of "HBV" target DNA shows a linear relationship between the fluorescence intensities and the concentration of target DNA from 0 to 200 nM ($R = 0.999$) with the detection limit of 5 nM (S/N = 3), and the RSD (relative standard deviation, $n = 5$) was less than 5%. The detection limit of each pair of split G-quadruplex probes is strongly related to the sensitivity of assembled G-quadruplex toward target DNA and fluorescence enhancement of small ligand. From the experimental results, it can be concluded that asymmetrically split probes (1:3) has better sensitivity than symmetrical probes, leading to a lower detection limit of asymmetrically split probes. It has been mentioned previously that the sensitivity of assembled G-quadruplex is influenced by various parameters, such as thermodynamic stabilities of three-way junctions, distinct architectural features of split G-quadruplex (Nakayama and Sintim, 2009).

Although there was no signal amplification, the sensitivity was comparable to those split peroxidase DNAzyme methods (Deng et al., 2008; Kolpashchikov, 2010; Qiu et al., 2011), and improved stability and reproducibility were obtained by fluorescent readout from G-quadruplex-binding dyes. In addition, the split strategy endowed our system extraordinary selectivity (Kolpashchikov, 2010), in contrast to other hybridization-based techniques, such as classical molecular beacons (Venkatesan et al., 2008; Wang et al., 2009). We also evaluated our probe design in the context in a diluted biological fluid (urine) and were able to detect the presence of HBV target in a 1% urine sample and could distinguish the single-point mutations from the perfectly complementary target under these conditions (Fig. S12).

4. Conclusions

In summary, we have completed a comprehensive investigation of three split probe designs via fluorescence readout of NMM. In all three cases, the sensitivity of target detection was highly dependent on the thermodynamic stability of the hybrid structure, which can be modulated by potassium ion concentrations. At high potassium concentrations, however, a loss in selectivity for cognate versus mismatched hybridization targets was observed. According to a comparison of our CD, fluorescence, and thermal data, the minimal concentration of potassium needed to fold the G-quadruplex at the three-way junction provides the optimal balance of sensitivity and selectivity of probe hybridization. Potassium concentrations that are above optimal cause the hybrid structures to be "too stable" to detect SNPs within the duplex regions at room temperature. The resulting optimized probes can detect SNPs with sensitivities comparable to those of binary probes (Grimes et al., 2010; Kolpashchikov, 2010; Qiu et al., 2011), and classical molecular beacons (Venkatesan et al., 2008; Wang et al., 2009) and could distinguish SNPs from the perfectly complementary targets in diluted biological fluids (Fig. S12). These results demonstrate how co-variation of probe design and potassium concentration can provide a powerful means to optimize G-quadruplex-mediated fluorescence readouts of duplex hybridization.

Acknowledgements

This work was supported by National Natural Science Foundation of China (No. 20905056 and 2011CB911000), the 973 Project (2009CB930100 and 2010CB933600), and the Swiss National Science Foundation (No. 130074).

Appendix A. Supplementary data

Supplementary data associated with this article can be found, in the online version, at doi:10.1016/j.bios.2011.10.038.

References

Alzeer, J., Vummidi, Balayeshwanth, R., Roth, Phillipe, J.C., Luedtke, Nathan, W., 2009. Angew. Chem. Int. Ed. 48, 9362–9365.
Arthanari, H., Basu, S., Kawano, T., Bolton, P., 1998. Nucleic Acids Res. 26, 3724–3728.
Bai, X., Shao, C., Han, X., Li, Y., Guan, Y., Deng, Z., 2010. Biosens. Bioelectron. 25, 1984–1988.
Bonanni, A., Pumera, M., Miyahara, Y., 2010. Anal. Chem. 82, 3772–3779.
Chang, C.-C., Kuo, I.C., Ling, I.F., Chen, C.-T., Chen, H.-C., Lou, P.-J., Lin, J.-J., Chang, T.-C., 2004. Anal. Chem. 76, 4490–4494.
D'Agata, R., Corradini, R., Ferretti, C., Zanoli, L., Gatti, M., Marchelli, R., Spoto, G., 2010. Biosens Bioelectron. 25, 2095–2100.

Deng, M., Zhang, D., Zhou, Y., Zhou, X., 2008. J. Am. Chem. Soc. 130, 13095–13102.
Elbaz, J., Moshe, M., Shlyahovsky, B., Willner, I., 2009. Chem. Eur. J. 15, 3411–3418.
Ferapontova, E.E., Hansen, M.N., Saunders, A.M., Shipovskov, S., Sutherland, D.S., Gothelf, K.V., 2010. Chem. Commun. 46, 1836–1838.
Grimes, J., Gerasimova, Y.V., Kolpashchikov, D.M., 2010. Angew. Chem. Int. Ed. 49, 8950–8953.
Guo, W., Yuan, J., Dong, Q., Wang, E., 2009. J. Am. Chem. Soc. 132, 932–934.
Häner, R., Biner, S.M., Langenegger, S.M., Meng, T., Malinovskii, V.L., 2010. Angew. Chem. Int. Ed. 49, 1227–1230.
Hejazi, M.S., Pournaghi-Azar, M.H., Ahour, F., 2010. Anal. Biochem. 399, 118–124.
Hu, D., Pu, F., Huang, Z., Ren, J., Qu, X., 2010. Chem. Eur. J. 16, 2605–2610.
Hud, N.V., Smith, F.W., Anet, F.A.L., Feigon, J., 1996. Biochemistry 35, 15383–15390.
Kim, S.K., Cho, H., Jeong, J., Kwon, J.N., Jung, Y., Chung, B.H., 2010. Chem. Commun. 46, 3315–3317.
Koeppel, F., Riou, J.-F., Laoui, A., Mailliet, P., Arimondo, P.B., Labit, D., Petitgenet, O., Helene, C., Mergny, J.-L., 2001. Nucleic Acids Res. 29, 1087–1096.
Kolpashchikov, D.M., 2008. J. Am. Chem. Soc. 130, 2934–2935.
Kolpashchikov, D.M., 2010. Chem. Rev. 110, 4709–4723.
Kuang, S.-Y., Jackson, P.E., Wang, J.-B., Lu, P.-X., Muñoz, A., Qian, G.-S., Kensler, T.W., Groopman, J.D., 2004. Proc. Natl. Acad. Sci. U.S.A. 101, 3575–3580.
Li, H., Rothberg, L.J., 2004. Anal. Chem. 76, 5414–5417.
Li, H., Sun, Z., Zhong, W., Hao, N., Xu, D., Chen, H.-Y., 2010a. Anal. Chem. 82, 5477–5483.
Li, T., Wang, E., Dong, S., 2010b. Anal. Chem. 82, 7576–7580.
Ma, D.-L., Che, C.-M., Yan, S.-C., 2009. J. Am. Chem. Soc. 131, 1835–1846.
Nakayama, S., Sintim, H.O., 2009. J. Am. Chem. Soc. 131, 10320–10333.
Pavlov, V., Xiao, Y., Gill, R., Dishon, A., Kotler, M., Willner, I., 2004. Anal. Chem. 76, 2152–2156.
Phan, A.T., Modi, Y.S., Patel, D.J., 2004. J. Am. Chem. Soc. 126, 8710–8716.
Qin, H., Ren, J., Wang, J., Luedtke, N.W., Wang, E., 2010a. Anal. Chem. 82, 8356–8360.
Qin, W.J., Yim, O.S., Lai, P.S., Yung, L.-Y.L., 2010b. Biosens. Bioelectron. 25, 2021–2025.
Qin, Y., Hurley, L.H., 2008. Biochimie 90, 1149–1171.
Qiu, B., Zheng, Z.-Z., Lu, Y.-J., Lin, Z.-Y., Wong, K.-Y., Chen, G.-N., 2011. Chem. Commun. 47, 1437–1439.
Ren, J., Qin, H., Wang, J., Luedtke, N., Wang, E., Wang, J., 2011. Anal. Bioanal. Chem. 399, 2763–2770.
Russ Algar, W., Massey, M., Krull, U.J., 2009. Trends Anal. Chem. 28, 292–306.
Sen, D., Gilbert, W., 1990. Nature 344, 410–414.
Song, J., Li, Z., Cheng, Y., Liu, C., 2010. Chem. Commun. 46, 5548–5550.
Tyagi, S., Kramer, F.R., 1996. Nat. Biotechnol. 14, 303–308.
Venkatesan, N., Jun Seo, Y., Hyean Kim, B., 2008. Chem. Soc. Rev. 37, 648–663.
Vialas, C., Pratviel, G., Meunier, B., 2000. Biochemistry 39, 9514–9522.
Wang, K., Tang, Z., Yang, Chaoyong J., Kim, Y., Fang, X., Li, W., Wu, Y., Medley, Colin D., Cao, Z., Li, J., Colon, P., Lin, H., Tan, W., 2009. Angew. Chem. Int. Ed. 48, 856–870.
Wang, X., Lou, X., Wang, Y., Guo, Q., Fang, Z., Zhong, X., Mao, H., Jin, Q., Wu, L., Zhao, H., Zhao, J., 2010. Biosens. Bioelectron. 25, 1934–1940.
Weizmann, Y., Cheglakov, Z., Willner, I., 2008. J. Am. Chem. Soc. 130, 17224–17225.
White, E.W., Tanious, F., Ismail, M.A., Reszka, A.P., Neidle, S., Boykin, D.W., Wilson, W.D., 2007. Biophys. Chem. 126, 140–153.
Xiao, Y., Pavlov, V., Gill, R., Bourenko, T., Willner, I., 2004. Chem. BioChem. 5, 374–379.
Xu, Q., Deng, H., Braunlin, W.H., 1993. Biochemistry 32, 13130–13137.
Yang, C.J., Lin, H., Tan, W., 2005. J. Am. Chem. Soc. 127, 12772–12773.
Yang, P., De Cian, A., Teulade-Fichou, M.-P., Mergny, J.-L., Monchaud, D., 2009. Angew. Chem. Int. Ed. 48, 2188–2191.
Zhang, C.-y., Hu, J., 2010. Anal. Chem. 82, 1921–1927.